

Effects of the nuclear transformation $^{111}\text{Ag}(\text{I})$ to $^{111}\text{Cd}(\text{II})$ in a single crystal of $\text{Ag}[^{111}\text{Ag}](\text{imidazole})_2\text{NO}_3$

Bjarne Hansen

Department of Physics, Royal Veterinary and Agricultural University, Frederiksberg, Denmark

Jens T. Bukrinsky

Bioinorganic Group, Department of Chemistry, Royal Veterinary and Agricultural University, Frederiksberg, Denmark

Lars Hemmingsen

Department of Physics, Royal Veterinary and Agricultural University, Frederiksberg, Denmark

Morten J. Bjerrum

Bioinorganic Group, Department of Chemistry, Royal Veterinary and Agricultural University, Frederiksberg, Denmark

Kulwant Singh

Department of Physics, Guru Nanak Dev University, Amritsar, India

Rogert Bauer*

Department of Physics, Royal Veterinary and Agricultural University, Frederiksberg, Denmark

(Received 6 November 1998)

Perturbed angular correlation of γ -ray (PAC) spectroscopy performed on a single crystal of $\text{Ag}(\text{imidazole})_2\text{NO}_3$ doped with radioactive $^{111}\text{Ag}(\text{I})$ reveals that one nuclear quadrupole interaction (NQI) characterizes the resulting PAC spectra. This implies a unique coordination geometry for $\text{Cd}(\text{II})$ after the decay of $^{111}\text{Ag}(\text{I})$. The full NQI tensor was determined in the experiment. The diagonal elements in the principal-axis system can be derived from the two parameters fitted to the spectrum: $\omega_0 = |\omega_{zz}| = 425.5 \pm 0.1$ Mrad/s and $\eta = |\omega_{xx} - \omega_{yy}| / |\omega_{xx} + \omega_{yy}| = 0.240 \pm 0.001$. Quantum-mechanical *ab initio* calculations of the NQI tensor using the known geometry of $\text{Ag}(\text{imidazole})_2\text{NO}_3$ substituting $\text{Ag}(\text{I})$ with $\text{Cd}(\text{II})$ at the position of $\text{Ag}(\text{I})$ do not agree with the experimentally derived NQI tensor. The coordination number is two for $\text{Ag}(\text{I})$ in $\text{Ag}(\text{imidazole})_2\text{NO}_3$, which is an unusual coordination number for $\text{Cd}(\text{II})$. The $\text{Cd}(\text{II})$ ion was therefore moved towards the NO_3^- anion in the *ab initio* calculations, in an attempt to include the two oxygen atoms of the nitrate ion in the coordination sphere. This resulted in a four coordinated structure with reasonable $\text{Cd}(\text{II})$ -ligand bond lengths. The *ab initio* calculations based upon this geometry agrees well with the experimentally determined NQI tensor. [S0163-1829(99)11021-X]

INTRODUCTION

In the present work the nuclear quadrupole interaction (NQI) in a single crystal of $\text{Ag}(^{111}\text{Ag})(\text{imidazole})_2\text{NO}_3$ was derived from perturbed angular correlation (PAC) spectroscopy. *Ab initio* calculations showed that most likely a change of coordination geometry occurred faster than 5 ns after the decay of $^{111}\text{Ag}(\text{I})$ to $^{111}\text{Cd}(\text{II})$. The choice of $\text{Ag}(^{111}\text{Ag})(\text{imidazole})_2\text{NO}_3$ for the present investigations was made to monitor possible changes in the metal coordination geometry after $\text{Ag}(\text{I})$ decays to $\text{Cd}(\text{II})$ by the β^- decay $^{111}\text{Ag}(\text{I}) \rightarrow ^{111}\text{Cd}(\text{II}) + \beta^-$ as shown in Fig. 1. In $\text{Ag}(\text{imidazole})_2\text{NO}_3$ the $\text{Ag}(\text{I})$ ion is linearly coordinated to two imidazoles, which is an unusual geometry for $\text{Cd}(\text{II})$. Consequently, structural changes are expected when $\text{Ag}(\text{I})$ is almost instantaneously changed into $\text{Cd}(\text{II})$ by a nuclear decay. Similar investigation performed on the copper protein azurin showed that the coordination geometry for $\text{Ag}(\text{I})$ relaxes to the geometry of $\text{Cd}(\text{II})$ on a time scale of about 100 ns at 25 °C.¹

Applying perturbed angular correlation of γ -ray (PAC) spectroscopy to a single crystal allows for the determination of the full nuclear quadrupole interaction (NQI) tensor in contrast to experiments on randomly oriented molecules, where only the eigenvalues of the tensor are obtained. Previous work on the determination of the NQI tensor has been performed with various experimental techniques including PAC, NMR, and electron-nuclear double resonance (ENDOR) spectroscopy.²⁻⁷ In the work by Menningen, Haas, and Rinneberg on ^{111m}Cd , ^{69}Ge , or ^{71}As impurities in orthorhombic Ga the total NQI tensor was determined with PAC spectroscopy in the presence of a magnetic field.^{2,3} The full tensor for the nuclei ^{111}In and ^{111m}Cd on a Pd(111) surface has been determined using PAC spectroscopy⁴ and for the nucleus ^{14}N in 2-aminoethyl hydrogen sulfate by single-crystal ENDOR spectroscopy.⁷ Using NMR Thomas Vosegaard *et al.* determined both the chemical-shielding anisotropy and the NQI tensor for ^{87}Rb in single crystals of RbClO_4 and Rb_2SO_4 , and for ^{71}Ga in a single crystal of $\text{Y}_3\text{Ga}_5\text{O}_{12}$.^{5,6}

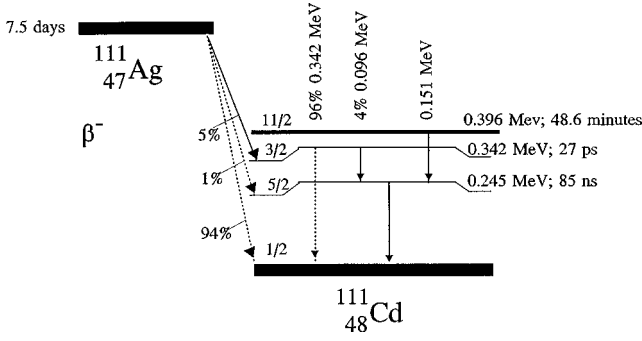


FIG. 1. Energy levels for the decay of ^{111}Ag to ^{111}Cd . The two γ rays detected in coincidence are the 96 keV transition (γ_1) and the 245 keV transition (γ_2). Note that only 5% of the ^{111}Ag nuclei decays to the excited state in ^{111}Cd with angular momentum of $\frac{3}{2}$. Of these only 4% decay through the double decay used for PAC spectroscopy.

SINGLE-CRYSTAL PAC THEORY

Single-crystal PAC spectroscopy provides the full NQI tensor $\underline{\omega}$, which is related to the electric-field gradient tensor \underline{V} , the quantity obtained from *ab initio* calculations by

$$\underline{\omega} = \frac{3\pi eQ}{10h} \cdot \underline{V}, \quad (1)$$

where Q is the magnitude of the nuclear quadrupole moment, e is the charge of a proton, and h is Planck's constant. Because the trace of $\underline{\omega}$ is zero only two, independent parameters are needed to characterize the diagonal elements. They are chosen as $\omega_0 = |\omega_{zz}|$ and $\eta = (\omega_{xx} - \omega_{yy})/\omega_{zz}$, assuming that the eigenvalues have been ordered $|\omega_{zz}| \geq |\omega_{yy}| \geq |\omega_{xx}|$. Furthermore, the orientation of the principal-axis system (where the tensor is diagonal) can be determined. The perturbed angular correlation function $W(i, t)$ can be written as⁸

$$W(i, t) \propto \sum_{k_1, k_2} A_{k_1}(1) A_{k_2}(2) [(2k_1 + 1)(2k_2 + 1)]^{-1/2} \times \sum_{N_1, N_2} G_{k_1 k_2}^{N_1 N_2}(t) Y_{k_1}^{N_1*}(\theta_{i1}, \varphi_{i1}) Y_{k_2}^{N_2}(\theta_{i2}, \varphi_{i2}), \quad (2)$$

where the index i denotes that γ_1 is emitted in the direction having polar coordinates θ_{i1} , φ_{i1} and γ_2 is emitted in the direction θ_{i2} , φ_{i2} . $A_{k_1}(1)$ and $A_{k_2}(2)$ are coefficients determined by properties of the nuclear states. From Siegbahn,⁹ we get

$$A_k(1) \approx \begin{cases} 0.3742 & k=2 \\ 0 & k=4, \end{cases} \quad A_k(2) \approx \begin{cases} -0.5345 & k=2 \\ -0.6172 & k=4 \end{cases} \quad (3)$$

neglecting mixed multipolarity. By definition $A_0(1) = A_0(2) = 1$. $Y_k^N(\theta, \varphi)$ are the spherical harmonics. $G_{k_1 k_2}^{N_1 N_2}(t)$ represents the perturbation from a NQI and can be written as

$$G_{k_1 k_2}^{N_1, N_2}(t) = \sum_{m_a, m_b} (-1)^{2I+m_a+m_b} [(2k_1 + 1)(2k_2 + 1)]^{1/2} \times \begin{pmatrix} I & I & k_1 \\ m'_a & -m_a & N'_1 \end{pmatrix} \begin{pmatrix} I & I & k_2 \\ m'_b & -m_b & N'_2 \end{pmatrix} \times D_{N_1, N'_1}^{k_1}(\alpha, \beta, \gamma) D_{N_2, N'_2}^{k_2}(\alpha, \beta, \gamma) \times \sum_{n, n'} \langle n | m_b \rangle \langle n | m_a \rangle \langle n' | m'_b \rangle \langle n' | m'_a \rangle e^{-2\pi i/\hbar(E_n - E_{n'})}, \quad (4)$$

where n and n' denotes eigenstate and eigenfunctions of the NQI Hamiltonian with the following matrix elements in the principal system: $H_{m, m} - H_{m', m'} = \pi \hbar \omega_0 (m^2 - m'^2)$ and $H_{m, m \pm 2} = \pi/6 \hbar \omega_0 [(\frac{3}{2} \mp m)(\frac{5}{2} \mp m)(\frac{7}{2} \pm m)(\frac{9}{2} \pm m)]^{1/2} \eta$ and

$$D_{N_1, N'_1}^{k_1*}(\alpha, \beta, \gamma) D_{N_2, N'_2}^{k_2}(\alpha, \beta, \gamma)$$

are the product of matrix elements describing the rotation by the Euler angles α , β , and γ from the crystal system, defined in materials and methods, to the principal system.

MATERIALS AND METHODS

Preparation of single and powder crystals of $\text{Ag}(\text{imidazole})_2\text{NO}_3$

$^{111}\text{Ag}(\text{I})$ was prepared as described in Bauer *et al.*¹ Small crystals of $\text{Ag}(\text{imidazole})_2\text{NO}_3$ were obtained from aqueous solution by mixing 1.2 g (0.007 mol) AgNO_3 in 10 ml water with 2.0 g (0.03 mol) imidazole in 10 ml of water. A white precipitate of silver oxide/silver hydroxide immediately appeared upon mixing of the two solutions. The solution was acidified with 6 M HNO_3 until a clear solution was obtained (around pH 7). Crystals of $\text{Ag}(\text{imidazole})_2\text{NO}_3$ normally precipitated in the dark within one hour. $\text{Ag}(\text{imidazole})_2\text{NO}_3$ crystals doped with $^{111}\text{Ag}(\text{I})$ were prepared by adding radioactive $^{111}\text{Ag}(\text{I})$ in 20–40 μl water to the acidified solution of AgNO_3 and imidazole before crystals of $\text{Ag}(\text{imidazole})_2\text{NO}_3$ began to precipitate. The stock solution for growing large crystals for single-crystal experiments was made by the addition of 5.992 g imidazole (0.088 mol) to 150 ml of water and adjusting pH to just below 7 with 6 M HNO_3 . To this solution was added 100 ml water containing 7.474 g AgNO_3 (0.044 mol). Finally pH was raised to 6.20 with 2–3 drops of 3 M NaOH giving a little white precipitate of silver oxide/silver hydroxide which dissolved within a few minutes.

Seeding crystals were obtained from a setup of 48 batches of 3 ml stock solution in two tissue culture plates (Linbro Research, USA). They were evaporated at room temperature in an exsiccator containing NaOH pellets for 48 h. Most of these batches resulted in a white precipitate and only one or two contained isolated crystals of good quality (1–5 mg each) which could be used for seeding experiments.

Large crystals for x-ray powder diffraction were grown to a size larger than 8 mm^3 by seeding of 1–5 mg single crystals in 3 ml stock solution in tissue culture plates with evaporation at room temperature for 3–5 days.

For single-crystal PAC experiments a seeding crystal (~ 2 mg) was placed in Elisa plates (Linbro Research, USA) adding 200 μ l 0.32 M Ag(imidazole)₂ pH 6.20 (prepared in the same way as the stock solution) followed by 90 μ l of doubly deionized water containing approximately 5 MBq carrier free ¹¹¹Ag(I). This solution was then evaporated for 15 h at room temperature in an exsiccator containing NaOH pellets. The resulting crystal had turned slightly brown and weighed approximately 25 mg.

Characterization of single and powder crystals of Ag(imidazole)₂NO₃

The actual single crystal used for PAC measurements was indexed at 122 K in a MoK α beam using a CAD4 diffractometer aiming the beam through the center of the crystal. The investigated crystal is orthorhombic within the space group $P2_12_12_1$ with cell parameters $a=4.97$ Å, $b=10.92$ Å, $c=17.98$ Å, $\alpha=90.38$, $\beta=90.9$, and $\gamma=90.2$ (unrefined). The CAD4 data were furthermore used to determine the alignment of the crystal axes in the PAC experiment.

X-ray powder diffraction data was obtained from samples of small crystals and from a powdered large single crystal (larger than $2 \times 2 \times 3$ mm) of Ag(imidazole)₂NO₃ placed in 0.3 mm capillary tubes using a STOE STADIP instrument (STOE and CIE GmbH). STOE's VISUAL X^{POW} (1995) program package (STOE and CIE GmbH) was used for the data treatment. The cell parameters for the single and powder crystal(s) were found to be the same within the uncertainties, $a=4.996(2)$, $b=10.930(2)$, $c=18.051(2)$ in Å, $\alpha=90$, $\beta=90$, $\gamma=90$ in degrees in agreement with the published crystal structure.¹⁰

PAC spectroscopy on a single crystal and on powder crystals of Ag(imidazole)₂NO₃

Before mounting and alignment of the single crystal doped with ¹¹¹Ag(I) used in the PAC experiment larger bulbs were removed from the crystal with a pincer and a needle. The crystal was further washed with 100 μ l deionized water followed by 500 μ l butanol and the crystal was finally dried with 200 μ l ether. The cleaned crystal contained approximately 35% of the total activity added. The crystal was glued to the end of a glass capillary with cyanoacrylate and fixed to a truncated cone. The PAC setup consists of six detectors in an octahedral geometry, defining a cube with one detector at the center of each side square and with the sample in the center of the cube. The glass capillary on the cone was aligned relative to the detectors. The orientation of the unit cell was obtained from x-ray-diffraction data on the single crystal used for the PAC measurement. Thereby, the orientation of the crystal system, relative to the detectors, was determined. From this the polar θ_i and azimuthal angles ϕ_i of the six detectors in the crystal system were calculated (see Table I). The uncertainty of the alignment of the glass capillary relative to the detectors results in an uncertainty in θ_i and ϕ_i . The Euler angles and ω_0 and η values presented in Table II are weighted averages given these uncertainties.

TABLE I. Polar coordinates for the six detectors as seen in the crystal system.

Detector	θ	ϕ
1	107.1	119.7
2	72.9	60.3
3	22.7	75.9
4	157.3	255.9
5	104.9	25.0
6	75.1	205.0

PAC measurements were also performed on samples (100–200 mg) of powder Ag(imidazole)₂NO₃ doped with ¹¹¹Ag(I) and kept in plastic tubes.

Data analysis

From the six detectors 30 coincidence spectra can be formed, here denoted $W(D_i, D_j, t)$ where D_i and D_j denotes detector i and j , counting coincidence events between γ_1 and γ_2 , respectively. Adding the equivalent spectra and normalizing to the number of spectra added, we get nine different spectra, three at 180° and six at 90° between D_i and D_j . Examples of a 180° spectrum is $[W(D_1, D_2, t) + W(D_2, D_1, t)]/2$ and of a 90° spectrum is $[W(D_1, D_3, t) + W(D_1, D_4, t) + W(D_2, D_3, t) + W(D_2, D_4, t)]/4$. Note that because of the A_{24} term [see Eq. (3)] $W(D_1, D_3, t)$ is different from $W(D_3, D_1, t)$. We denote these nine spectra $\langle W(i, t) \rangle$, $i=1 \cdots 9$ where $\theta=180^\circ$ for $i=1 \cdots 3$ and $\theta=90^\circ$ for $i=4 \cdots 9$. These spectra were corrected for the background due to random coincidences $\langle B_i \rangle$ and weighted according to the left-hand side of Eq. (5), and then fitted with the function on the right-hand side of Eq. (5):

$$\frac{\langle W(i, t) \rangle - \langle B_i \rangle}{\langle \epsilon_i \rangle e^{-t/\tau_n} (1 + td \langle \epsilon_i \rangle / dt)} - 1 = \sum_{k=0,1,2,3} b_k(\tau_0) a_k(i) e^{-1/2(\omega_k \delta t)^2}, \quad (5)$$

where the amplitude $\langle \epsilon_i \rangle$ is a function of the efficiencies and solid angles of the involved detectors. The term $1 + td \langle \epsilon_i \rangle / dt$ accounts for a variation in time of the detector efficiencies, τ_n is the half-life of the $I = \frac{5}{2}$ state, $b_k(\tau_0) = \exp(-\omega_k^2 \tau_0^2 / 16 \ln 2)$ accounts for the finite time resolution τ_0 of the instrument, and ω_k are the three angular frequencies corresponding to the energy differences $2\pi(E_n - E_{n'})/h$ where E_n are the sublevels of the intermediate nuclear level in the $\gamma_1 - \gamma_2$ cascade. Small variations in the metal-ligand configuration in the different $[\text{Cd}(\text{imidazole})_2\text{NO}_3]^+$ units are accounted for by a Gaussian frequency distribution expressed by the term $\exp(-2\omega_k^2 \delta^2 t^2)$ term where δ represents the relative width of the distribution. The coefficients $a_k(i)$ are [see Eqs. (2), (4), and (5)]

TABLE II. The derived experimental parameters from PAC experiments with $\text{Ag}(\text{imidazole})_2\text{NO}_3$ crystals and the results from *ab initio* calculations, χ_r^2 are reduced chi-square values from the fitting to the PAC time spectra. The energies given are relative to geometry *A* (with similar condition for the surrounding point charges). Geometry *A'* represents a slight optimization of the original geometry *A* as explained in materials and method. Calculations indexed with *Q* include the CHELPG point charges. The uncertainty in η and ω_{zz} and Euler angles are estimated as described in the materials and methods section. For all geometries, a χ^2 value is given in the last column and formed as the squared sum of differences between theoretical and experimental values of η , ω_{zz} , α , β , and γ weighted by the respective uncertainty.

		Experimental data:					
		δ	η	$\omega_{zz}(\text{Mrad/s})$			χ_r^2
Powder		0.003 ± 0.002	0.236 ± 0.002	424.6 ± 0.2			0.99
single crystal		0.006 ± 0.001	0.240 ± 0.001	425.5 ± 0.1			1.15
		Q_{22}	Q_{24}	α_0	β_0	γ_0	
Single crystal		0.30 ± 0.01	0.15 ± 0.01	$17 \pm 6^\circ$	$128 \pm 1^\circ$	$89 \pm 14^\circ$	
		Calculated data:					
Geometry	Energy (kJ/mol)	η	ω_{zz} (Mrad/s)	α	β	γ	χ^2
<i>A</i>	0	0.21 ± 0.07	674 ± 80	4 ± 1	133 ± 1	86 ± 54	21
<i>A'</i>	-1.6	0.21 ± 0.07	672 ± 79	4 ± 1	133 ± 1	86 ± 54	21
<i>B</i>	-20.5	0.38 ± 0.09	489 ± 57	14 ± 2	130 ± 1	94 ± 5	4
<i>C</i>	-27.4	0.60 ± 0.07	424 ± 53	13 ± 2	129 ± 1	94 ± 2	28
<i>D</i>	-33.5	0.95 ± 0.04	319 ± 44	3 ± 7	60 ± 37	321 ± 74	321
<i>A_Q</i>	0	0.18 ± 0.06	709 ± 81	4 ± 1	133 ± 1	61 ± 69	31
<i>A'_Q</i>	-2.1	0.18 ± 0.06	704 ± 81	4 ± 1	133 ± 1	61 ± 69	31
<i>B_Q</i>	-10.6	0.23 ± 0.10	538 ± 61	13 ± 2	130 ± 1	91 ± 16	6
<i>C_Q</i>	-15.0	0.41 ± 0.09	480 ± 57	13 ± 2	130 ± 1	94 ± 4	7
<i>D_Q</i>	-17.0	0.78 ± 0.05	373 ± 49	14 ± 2	131 ± 1	101 ± 2	123
Euler angles for the vector $\mathbf{u}(\text{N11}) - \mathbf{u}(\text{N21})$:							
<i>A</i>				4	133		
<i>B</i>				9	131		
<i>C</i>				9	130		
<i>D</i>				8	132		

$$a_k(i) = \left(\begin{array}{l} Q_{22} A_{22} \frac{1}{5} \sum_{N1, N2} G_{22}^{0N1N2}(\omega_k) Y_2^{N1*}(\theta_{i1}, \varphi_{i1}) Y_2^{N2}(\theta_{i2}, \varphi_{i2}) \\ + Q_{24} A_{24} \frac{1}{\sqrt{45}} \sum_{N1, N2} G_{24}^{0N1N2}(\omega_k) Y_2^{N1*}(\theta_{i1}, \varphi_{i1}) Y_4^{N2}(\theta_{i2}, \varphi_{i2}) \end{array} \right). \quad (6)$$

Q_{22} and Q_{24} represent detector solid angle corrections. The index 0 on G denotes the time independent part. The two sets $\{\theta_{1,i}, \phi_{1,i}\}$ and $\{\theta_{2,i}, \phi_{2,i}\}$ are the polar angles in the crystal coordinate system for γ_1 and γ_2 , respectively.

In the case of powder material the experimental spectrum is constructed [see Eqs. (2) and (4)] according to the right-hand side of Eq. (7) and then fitted with the function on the left-hand side of Eq. (7):

$$\frac{1}{5} \sum_N A_{22} Q_{22} G_{22}^{NN}(t) = 2 \frac{\langle W(180^\circ, t) \rangle - \langle W(90^\circ, t) \rangle}{\langle W(180^\circ, t) \rangle + 2 \langle W(90^\circ, t) \rangle}. \quad (7)$$

$\langle W(180^\circ, t) \rangle$ denotes the sixth root of the product of the six experimental 180° spectra (these are all equivalent for pow-

der material) after background subtraction and zero-point adjustment, and $\langle W(90^\circ, t) \rangle$ denotes the 24th root of the product of the 24 experimental 90° spectra.

Using the fitted NQI ω_0 , η , and δ parameters from powder $\text{Ag}(\text{imidazole})_2\text{NO}_3$, each of the nine single-crystal spectra were least-square fitted, to find values for $\langle \epsilon_i \rangle$, $\langle B_i \rangle$, $d\langle \epsilon_i \rangle/dt$, $a_k(i)$, Q_{22} , and Q_{24} using the fit function given in Eq. (5). τ_0 was estimated to be 1.5 ns based upon a ^{75}Se time calibration. Prompt coincidences (i.e., coincidences where the two γ rays are detected simultaneously) between Compton scattered γ rays from the dominant (96%) transition between the spin $\frac{3}{2}$ and $\frac{1}{2}$ nuclear states (Fig. 1) restricted the useful time range to be above 5.6 ns. The half-life of 84 ns for the intermediate level sets a practical upper limit, here taken as 230.4 ns. The fitted values of $a_k(i)$ can then be used

to determine the Euler angle describing the rotation from the crystal system to the principal-axis system with the help of Eqs. (4) and (6). However, for $\text{Ag}(\text{imidazole})_2\text{NO}_3$ in the space group $P2_12_12_1$, there are four molecules in one unit cell, thus requiring four sets of Euler angles. These are: $\Omega_0 = (\alpha_0, \beta_0, \gamma_0)$, $\Omega_x = (-\alpha_0, \beta_0 + \pi, \gamma_0)$, $\Omega_y = (\pi - \alpha_0, \beta_0 + \pi, \gamma_0)$, and $\Omega_z = (\pi + \alpha_0, \beta_0, \gamma_0)$. Identical contributions are obtained when Ω_0 or Ω_z and when Ω_x or Ω_y are inserted for the Euler angles in Eq. (4). Thus the addition of a contribution from Ω_0 and Ω_x in Eq. (4) is sufficient.

Ab initio calculation on different $[\text{Cd}(\text{imidazole})_2\text{NO}_3]^+$ geometries

The quantum chemical calculations of energies and electric-field gradients (EFG's) were performed using second order Moller-Plesset perturbation theory (MP2), freezing core orbitals on the H, C, N, and O atoms and $1s2s2p3s3p3d$ on cadmium and silver. The calculation of a grid of point charges representing the surrounding molecules in the crystal were performed on the $\text{Ag}(\text{imidazole})_2\text{NO}_3$ complex at the level of MP2. The charges assigned to the atoms were calculated using charges fitted to the electrostatic potential (CHELPG) procedure.¹¹ Preliminary charges for all atoms in the basic $\text{Ag}(\text{imidazole})_2\text{NO}_3$ unit in the gas phase were calculated. Next, all atoms in the surrounding units with a distance to Ag less than 21 Å were taken into account. These atoms were ascribed fixed point charges equal to the gas phase charges. In the next iterative step we used the corrected charges in the basic unit as the fixed point charges at the surrounding atoms, etc. The charges converged within $0.01e$ after four steps. The basis sets used were $6-31G(d)$ for all H, C, N, and O atoms,¹²⁻¹⁷ the $[19s15p9d4f/11s9p5d2f]$ polarized basis set for cadmium of Kellö and Sadlej¹⁸ and the uncontracted $[17s12p8d]$ basis set for silver of Gropen.¹⁹ A value of $0.83b$ was used for the nuclear quadrupole moment.²⁰ Based on previous work^{21,22} we use an uncertainty of 20% on the eigenvalues of the EFG tensor. The calculations were performed on a Silicon Graphics Origin 200 with a 180 Mhz MIPS R10000 processor, using the program package GAUSSIAN94.²³

Coordinates for the atoms in the $\text{Ag}(\text{imidazole})_2\text{NO}_3$ structure, except the hydrogen atoms, are from Antti and Lundberg¹⁰ (see Table III, and Fig. 2). The H atom connected to atom C11, denoted H11, is positioned on the bisecting-line of C11 (the line bisecting the angle N11-C11-O12); the positions of the other H atoms are determined in the same way. The distances $d(\text{H},\text{N})=1.05$, $d(\text{H},\text{C})=1.09$ Å have been used. Hydrogen bonds exist to atoms outside this basic $\text{Ag}(\text{imidazole})_2\text{NO}_3$ unit: N12-H1 \cdots O2', N22-H2 \cdots O3', N22'-H2' \cdots O3 and N12'-H1' \cdots O2, where the primed atoms belong to other $\text{Ag}(\text{imidazole})_2\text{NO}_3$ units.

The possibility for changes in the coordination geometry following the decay of the Ag nucleus was investigated performing *ab initio* calculations on different plausible geometries. In these Cd(II) was moved towards the NO_3^- group.

Significant differences in bond lengths and angles exist between the two imidazole rings using the coordinates in the $\text{Ag}(\text{imidazole})_2\text{NO}_3$ structure; for example C11-C12, C21-C22 are 1.335, 1.385 Å and C12-N12, C22-N22 are 1.387, 1.422 Å and N12-C13, N22-C23 are 1.364, 1.307 Å, respectively. We have therefore modified this structure such that

the distances and angles in both rings are the same. The values were: C11-C12=1.375 Å, C21-C22=1.375 Å, C12-N12=1.405 Å, C22-N22=1.405 Å, N12-C13=1.330 Å and N22-C23=1.330 Å. With different fixed Cd(II) positions closer to the NO_3^- group than in the $\text{Ag}(\text{imidazole})_2\text{NO}_3$ geometry, the two imidazole rings were rotated and translated simultaneously to minimize the rms value of the distances from the original geometry for the six carbon and four nitrogen atoms in the imidazole rings. Distances from Cd(II) to N11 or N21 of approximately 2.26 Å and distances for N12-O2' and N22-O3' of approximately 2.88 Å together with approximately 180° for the angles N12-H1-O2', N22-H2-O3' were attempted for optimum hydrogen bonding. Apart from the original geometry A [the geometry with Cd(II) at the Ag(I)-position] three other geometries were chosen: B, C, and D (with Cd(II) moved respectively 0.456, 0.598, 0.789 Å). Table IV shows some selected angles and distances. Notice the values of rms (defined in the table caption), respectively 0.335, 0.341, 0.384 Å. The bond angles for the imidazole rings are nearly optimal for all geometries: the angle between the vector connecting N11 or N21 with Cd(II) and the corresponding bisecting line for each nitrogens are less than 9°. In the extreme geometry D, the ligand to Cd(II) distances approaches those observed for other compounds.²⁴ Figure 3 shows geometries A and B.

It is clear from the dihedral angles H1'-O2-N3-O1 of 7.0° and H2'-O3-N3-O1 of 9.5° that H1' and H2' are nearly in the plane of the NO_3^- group, and furthermore O3-N3-H2' = 108.8°, O2-N3-H1' = 106.0°. The H1' and H2' are on the same side of this plane, while the Cd atom is located on the other side with dihedral angles: Cd-O2-N3-O1 from 22.9–26.5°, Cd-O3-N3-O1 from 23.5–28.6°. This stabilizes the position and orientation of the NO_3^- group. Moving the Cd(II) ion will disturb this balance, but substantial change in the position and orientation of the plane probably involves the breaking of at least one of the hydrogen bonds to H1' or H2'. It is thus very difficult to estimate the limits for moving the cadmium and this point has not been further investigated. In all geometries the positions of the atoms in the NO_3^- group were fixed to the position used for geometry A. The distance between the cadmium atom in geometry A and atoms in other NO_3^- groups or in other imidazole rings is at least 5 Å, and we have ignored any changes in partial charges or positions in other units.

RESULTS

PAC experiments

Figure 4 shows the anisotropy as a function of time and the Fourier transforms of the nine PAC spectra from the single-crystal experiment. Despite the recoil energy of the $^{111}\text{Cd}(\text{II})$ nucleus after the decay $^{111}\text{Ag}(\text{I}) \rightarrow ^{111}\text{Cd}(\text{II})^{111} + \beta^-$, estimated to be less than 79 kcal/mol,¹ we can conclude that all $^{111}\text{Cd}(\text{II})$ ions are in the same geometry in the time interval where our PAC spectra are analyzed, that is 5–200 ns after the decay (Fig. 4 and Table II). This geometry is very rigid as evidenced by the low value for δ (Table II).

Table II shows the selected parameters derived from the powder spectrum as well as the parameters from the experiments on the single crystal (in both cases the detector-crystal

TABLE III. Coordinates (in Å) for the atoms in the unit cell of $\text{Ag}(\text{imidazole})_2\text{NO}_3$ in geometry *A* and *B* (see text) and the calculated CHELPG charges (in elementary charge) for coordination geometry *A* with $\text{Ag}(\text{I})$ (these values are the point charges at surrounding atoms used in the calculations A_Q , B_Q , C_Q , and D_Q).

	<i>x</i>	<i>y</i>	<i>z</i>	Q		<i>x</i>	<i>y</i>	<i>z</i>
Geometry <i>A</i>					Geometry <i>B</i>			
Ag(I)	0.752	1.922	0.259	0.447	Cd(II)	0.500	2.300	0.300
N11	2.383	1.944	-1.092	-0.218	N11	2.379	2.269	-0.941
C11	3.509	1.166	-1.056	-0.105	C11	3.273	1.251	-1.079
C12	4.373	1.583	-1.985	-0.081	C12	4.236	1.572	-2.007
N12	3.784	2.658	-2.635	-0.224	N12	3.880	2.860	-2.438
C13	2.569	2.843	-2.044	0.015	C13	2.782	3.212	-1.775
N21	-0.711	1.750	1.800	-0.241	N21	-0.890	1.742	1.887
C21	-0.933	0.774	2.720	-0.156	C21	-1.121	0.605	2.598
C22	-1.946	1.177	3.576	-0.107	C22	-2.096	0.837	3.540
N22	-2.295	2.474	3.109	-0.233	N22	-2.457	2.183	3.372
C23	-1.549	2.740	2.069	0.128	C23	-1.714	2.669	2.383
H11	3.675	0.332	-0.372	0.132	H11	3.232	0.311	-0.529
H12	5.355	1.158	-2.193	0.164	H12	5.081	0.966	-2.333
H1	4.182	3.224	-3.424	0.395	H1	4.360	3.467	-3.148
H13	1.854	3.619	-2.316	0.177	H13	2.273	4.167	-1.904
H21	-0.399	-0.174	2.775	0.162	H21	-0.610	-0.344	2.444
H22	-2.375	0.627	4.413	0.166	H22	-2.502	0.128	4.262
H2	-3.009	3.146	3.482	0.396	H2	-3.172	2.738	3.904
H23	-1.609	3.663	1.493	0.150	H23	-1.769	3.696	2.021
N3	0.580	5.313	-0.061	1.074	N3	0.580	5.313	-0.061
O1	0.909	6.417	-0.504	-0.668	O1	0.909	6.417	-0.504
O2	-0.406	4.723	-0.465	-0.679	O2	-0.406	4.723	-0.465
O3	1.243	4.785	0.842	-0.694	O3	1.243	4.785	0.842
Position of atoms in other unit cells involved in hydrogen bonding:								
O2'	5.057	4.384	-4.534					
O3'	-4.220	4.322	4.157					
N22'	3.169	6.634	1.890					
H2'	2.476	6.032	1.493					
N12'	-1.679	6.450	-2.364					
H1'	-1.291	5.918	-1.611					

distance is 16.4 mm). In all fits a least-square χ^2 search has been applied. The uncertainties given for the Euler angles includes uncertainties from the limited precision in mounting the crystal holder. The fitted NQI parameters (η , ω_{zz} , δ) were almost identical in the two experiments.

Ab initio calculations

Ab initio quantum-mechanical calculations, with partial charges at the surrounding atoms included and excluded, respectively, were performed on five geometries: *A* (the original, the geometry with Cd(II) at the Ag(I) position), *A'* the structure modified to give the same bond distances within the two imidazole rings, and geometries *B*, *C*, and *D*, with Cd(II) moved 0.456, 0.598, and 0.789 Å, towards the NO_3^- group. The positions of the two imidazole units were slightly adjusted in *B*, *C*, and *D* to facilitate favorable bonding angles to Cd(II). The influence on the $[\text{Cd}(\text{imidazole})_2\text{NO}_3]^+$ complex from the neighbor $\text{Ag}(\text{imidazole})_2\text{NO}_3$ units is threefold: (1) A direct contribution to the EFG at the cadmium position, (2) polarization of the electronic charge density, and (3) the

presence of four hydrogen bonds to atoms in other units, which is represented by partial charges on the atoms in the surrounding $\text{Ag}(\text{imidazole})_2\text{NO}_3$ units.

Table II shows the calculated energy, η , ω_{zz} , and the Euler angles for the principal-axis system for the different geometries. The standard deviations on all parameters are crude estimates. Notice that, for a certain geometry, the calculated Euler angles are nearly independent of whether point charges are included or not. \mathbf{z}_p and \mathbf{y}_p have been interchanged in the calculated result for geometry *D*, indicating a strong interaction between the cadmium atom and the NO_3^- group.

The differences in the calculated energies between geometry *A*, *B*, *C*, and *D*, although small, indicate an attraction between Cd(II) and the NO_3^- group, favoring a movement of Cd(II) towards the NO_3^- group. Note that a full geometry optimization was not performed. In all calculations, except for geometry *D*, the calculated *z*-principal axis almost coincides with the vector between the two coordinating nitrogen atoms [$\mathbf{z}_p \approx \mathbf{u}(\text{N11}) - \mathbf{u}(\text{N21})$], confer with Table II, and for

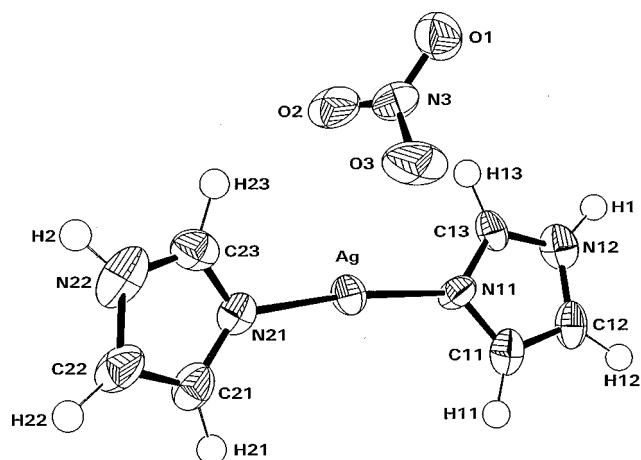


FIG. 2. Oak Ridge Thermal Ellipsoid Plot Program (ORTEP) drawing of one formula unit of $\text{Ag}(\text{imidazole})_2\text{NO}_3$ with the atom numbering used throughout the text. The atoms, except for hydrogen atoms, are represented as 50% probability ellipsoids. Coordinates and anisotropic vibrational parameters, except for hydrogen atoms, are taken from Ref. 10. Coordinates for hydrogen atoms are estimated (see text), and represented as spheres with a radius of 0.15 Å.

the x principal axis $\mathbf{x}_p \propto \mathbf{u}(\text{O}2) + \mathbf{u}(\text{O}3)$ [$\mathbf{u}(l)$ is the unit vector from cadmium to atom l]. Figure 3 shows geometry B with calculated principal axis (for calculation B_Q).

From Table II it can be seen that the effect of charge inclusion is a lowering of η and an increase of ω_0 . The calculated value for η and the Euler angles in geometry A is close to the experimental value, except for a minor discrepancy in the α angle. However, the calculated value for ω_0 is far too high. For geometry B and C the calculated values for η and ω_0 and the three Euler angles are close to the experimental values. The calculated values for geometry D do not agree in the value for η and the values for the Euler angles.

TABLE IV. Selected distances in Å and angles in degrees for the different geometries together with root-mean-square deviation (rms) in Å in positions of the C and N atoms in the two imidazole rings relative to geometry A .

Geometry	A	B	C	D
rms	0.000	0.335	0.341	0.384
Cd(II)-N11	2.118	2.252	2.239	2.277
Cd(II)-N21	2.132	2.182	2.210	2.250
Cd(II)-O2	3.116	2.698	2.543	2.353
Cd(II)-O3	2.963	2.650	2.485	2.313
N11-Cd(II)-N21	172.1	158.2	153.8	149.9
N11-Cd(II)-O2	97.4	97.8	102.0	104.5
N11-Cd(II)-O3	89.3	83.8	86.9	93.3
N21-Cd(II)-O2	89.2	102.8	104.0	104.7
N21-Cd(II)-O3	92.8	105.6	107.2	109.8
O2-Cd(II)-O3	40.4	46.4	49.5	53.6
Cd(II)-O3-N3	100.4	95.8	94.3	91.6
Cd(II)-O2-N3	93.3	94.0	92.0	90.2

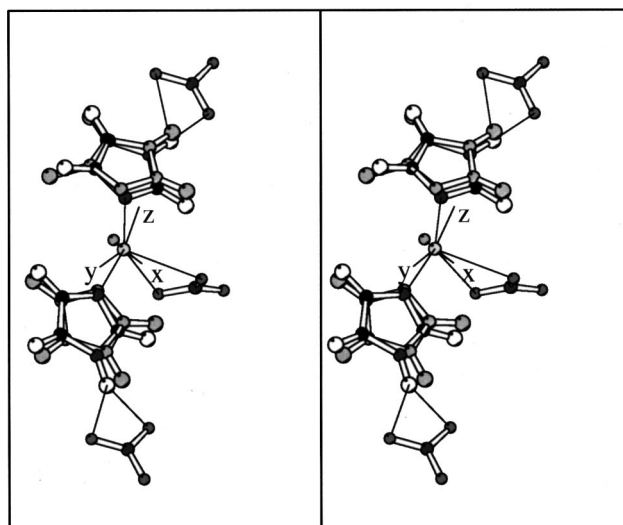


FIG. 3. Stereo view of the proposed geometry of $[\text{Cd}(\text{imidazole})_2\text{NO}_3]^+$ (geometry B). The two NO_3^- groups, which are hydrogen bonded to the imidazole rings, are from asymmetric units related by symmetry. Metal-ligand interactions and hydrogen bonds in the Cd(II) model are indicated with thin lines and the original structure of $\text{Ag}(\text{imidazole})_2\text{NO}_3$ (geometry A) is indicated with gray shading the atoms. The x , y , and z axes represent the experimentally determined principal axis.

X-ray diffractions

Both the powder material and the single crystal have identical cell parameters within the uncertainties. These results are furthermore in reasonable accordance with the published crystal structure.¹⁰

DISCUSSION

Linear imidazole coordination for Cd(II) with a very short bond length for the Cd(II)-N(imidazole) bond of 2.1 Å is unusual and will likely result in a nonequilibrium state for Cd(II) after the decay from $^{111}\text{Ag}(\text{I})$ to $^{111}\text{Cd}(\text{II})$. Cd(II) is more likely to prefer a higher coordination number such as 4 and the Cd(II)-N(imidazole) and the Cd(II)-O(NO_3^-) bonding distance is expected to be approximately 2.25–2.35 Å and 2.34–2.60 Å, respectively.²⁵ The Ag(I)-N(imidazole) and the Ag(I)-O(NO_3^-) bonding distances are found to be 2.1 Å and 3.0 (and 3.1) Å, respectively, in the $\text{Ag}(\text{imidazole})_2\text{NO}_3$ structure (see Table IV). This is likely to produce an energetic constraint which could be released by repositioning Cd(II) to a four coordinated geometry if the energy gained by this is large compared to the energy cost arising from the local change in crystal packing it induces.

We have therefore proposed a change from the linear imidazole coordination with Ag(I) to a four coordinated Cd(II) geometry with two nitrogen from imidazole and two oxygen from the NO_3^- group as ligands. This proposal can explain the fact that the experimental value of the asymmetry parameter η is higher than expected in an almost linear geometry. The central feature in the geometries tested in this work (see Table III) involves a movement of the Cd(II) towards the nitrate ion, which is fixed, followed by relaxation of the two imidazole rings. From Table IV, it is seen that the Cd(II)-ligand distances are within the expected range in the geom-

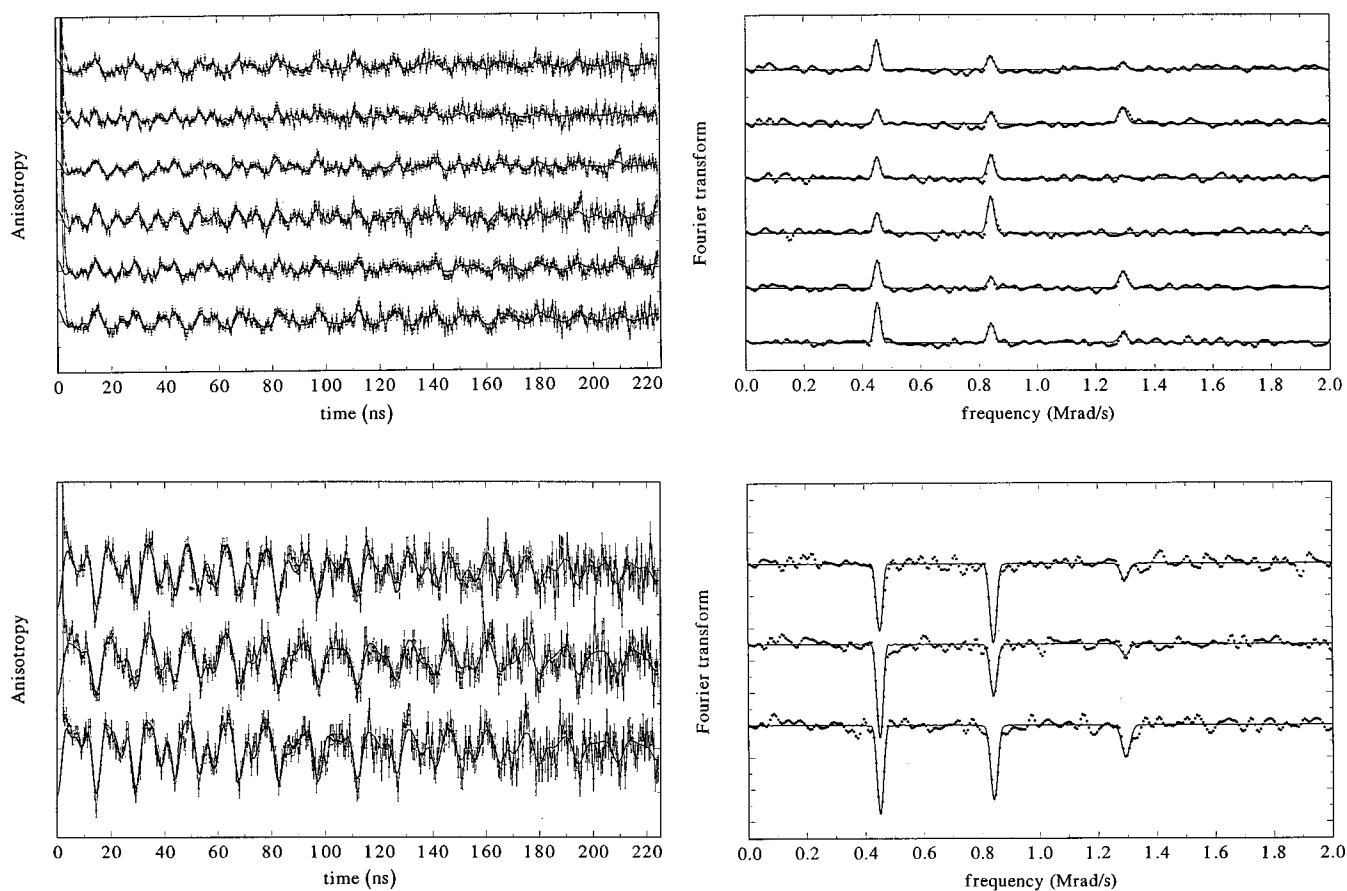


FIG. 4. Anisotropy as a function of time and the Fourier transforms (arbitrary unit on y axes) of the nine different single-crystal spectra, constructed as described by Eq. (5). The panels with three curves are 180° spectra and those with six, the 90° spectra. The orientation of the principal system is determined by the 27 cosine amplitudes $a_k(i)$.

etries B , C , and D . It is clear that the calculated value of ω_0 and α in geometry A and A_Q disagrees significantly with the experimental values obtained from the PAC experiment (Table II). Calculations performed with Ag(I) in geometry A instead of Cd(II) gives almost identical NQI parameters with the exception of an ω_0 value of 524 Mrad/s. However, the difference in electronic structure between Ag(I) and Cd(II) is expected to relax within a few ps (Ref. 26) such that the relevant ω_0 value reflected in the PAC time spectra will be that calculated for Cd(II). The geometries C , D , and D_Q are also excluded because of the high values calculated for η . The best agreement between the results from the *ab initio* calculations including charges, and the results from the single-crystal PAC experiment, is obtained by either geometry B_Q or C_Q (Table II). The decrease in energy observed for the tested geometries, relative to the energy of Cd(II) in the Ag(I) geometry (A_Q or A'_Q), is largest from A'_Q to B_Q and insignificant from C_Q to D_Q . Combining the values for the χ^2 with the value for the energy the most probable geometry would be C_Q . For this geometry, most of the strain on the Cd(II) complex is released relative to the geometry denoted A'_Q . However, it should be noted that no energy optimization of the changed geometries have been performed, because the effect of crystal packing is unknown. We conclude that most likely a stable (or metastable) $[\text{Cd}(\text{imidazole})_2\text{NO}_3]^+$ complex is formed after the decay of Ag(I) to Cd(II) with a ligand geometry, which is different from the

Ag(imidazole) $_2$ NO $_3$ complex. This new conformation is fully established within 10–20 ns. However, it cannot be excluded that further structural rearrangements occur μs after, as the time scale of the PAC spectrum is from 10–250 ns after the decay. A relaxation of a Ag(I) geometry in to a Cd(II) geometry has also been observed in the copper protein, azurin, within a time scale of about 100 ns.¹ The present study is the first time that the full NQI tensor has been determined for a Cd(II) complex experimentally as well as by *ab initio* calculations. Perspectives includes PAC experiments on single crystals of metal containing proteins, providing the full NQI tensor, thereby increasing the information content. In addition, we have seen that the *ab initio* calculations provide a NQI tensor, which is in surprisingly good quantitative agreement with the experimentally determined NQI tensor. To exploit the results from a single-crystal PAC experiment fully, knowledge of an accurate coordination geometry both of the Cd(II) and of the Ag(I) complex, is needed. It is not possible to obtain this information from x-ray diffraction on a system with a relatively small ligand (small molecule like Ag(imidazole) $_2$ NO $_3$). The Cd(imidazole) $_2$ NO $_3^+$ complex is only present in trace amounts and the structure is therefore not likely to be independent of the Ag(imidazole) $_2$ NO $_3$ structure. In a system with a large ligand, like a metal containing protein, the coordination of a metal ion in one molecule in a crystal is most likely independent of the metal coordination in the other molecules in the crystal. The structural knowl-

edge could thus be collected from each species independently.

ACKNOWLEDGMENTS

We thank Dr. Peter Andersen, University of Copenhagen for help with the x-ray powder diffraction, Marianne L.

Jensen, Agricultural University of Copenhagen, for her skillful help with sample preparations and Flemming Hansen, University of Copenhagen, for his help with indexing the single crystal on the CADY diffractometer. The work was supported by grants from the Danish Natural Science Research Council (through the Centre for Bioinorganic Chemistry).

- *Author to whom correspondence should be addressed. Present address: Department of Physics, Royal Veterinary and Agricultural University, Thorvaldsensvej 40, DK-1871 Frederiksberg C, Denmark; FAX: +45 35282350; electronic address: roger@kvlvax.kvl.dk
- ¹R. Bauer, E. Danielsen, L. Hemmingsen, M. J. Bjerrum, Ö. Hansson, and K. Singh, *J. Am. Chem. Soc.* **119**, 157 (1997).
- ²M. Menningen, H. Hass, and H. Rinneberg, *Phys. Rev. B* **35**, 8378 (1987).
- ³M. Menningen, H. Hass, O. Echt, *et al.* *Phys. Rev. B* **35**, 8385 (1987).
- ⁴E. Hunger, H. Hass, and H. Grawe, *Hyperfine Interact.* **60**, 999 (1990).
- ⁵T. Vosegaard, J. Skibsted, H. Bildsøe, and H. J. Jacobsen, *J. Magn. Reson., Ser. A* **122**, 111 (1996).
- ⁶T. Vosegaard, D. Massiot, N. Gautier, and H. J. Jacobsen, *Inorg. Chem.* **36**, 2446 (1997).
- ⁷A. R. Sørnes, E. Sagstuen, and A. Lund, *J. Phys. Chem.* **99**, 16 867 (1995).
- ⁸B. Tilman, *Hyperfine Interact.* **52**, 189 (1989); **73**, 387 (1992).
- ⁹*Alpha-, Beta- and Gamma-ray Spectroscopy*, edited by K. Siegbahn (North-Holland, Amsterdam, 1965), Vol. 2.
- ¹⁰Carl-Johan Antti and B. K. S. Lundberg, *Acta Chem. Scand.* **25**, 1758 (1971).
- ¹¹C. M. Breneman and K. B. Wiberg, *J. Comput. Chem.* **11**, 361 (1990).
- ¹²R. Ditchfield, W. J. Hehre, and J. A. Pople, *J. Chem. Phys.* **54**, 724 (1971).
- ¹³W. J. Hehre, R. Ditchfield, and J. A. Pople, *J. Chem. Phys.* **56**, 2257 (1972).
- ¹⁴P. C. Hariharan and J. A. Pople, *Mol. Phys.* **27**, 209 (1974).
- ¹⁵M. S. Gordon, *Chem. Phys. Lett.* **76**, 163 (1980).
- ¹⁶P. C. Hariharan and J. A. Pople, *Theor. Chim. Acta* **28**, 213 (1973).
- ¹⁷M. M. Francl, W. J. Pietro, W. J. Hehre, J. S. Binkley, M. S. Gordon, D. J. Defrees, and J. A. Pople, *J. Chem. Phys.* **77**, 3654 (1982).
- ¹⁸V. Kelloe and A. J. Sadlej, *Theor. Chim. Acta* **91**, 353 (1995).
- ¹⁹O. Gropen, *J. Comput. Chem.* **8**, 982 (1987).
- ²⁰P. Herzog, K. Freitag, M. Reuschenbach, and H. Walitzki, *Z. Phys. A* **294**, 13 (1980).
- ²¹L. Hemmingsen and U. Ryde, *J. Phys. Chem.* **100**, 4803 (1996).
- ²²L. Hemmingsen, U. Ryde, and R. Bauer (unpublished).
- ²³A. M. Frisch, G. W. Trucks, H. B. Schlegel, P. M. W. Gill, B. G. Johnson, M. A. Robb, J. R. Cheeseman, G. A. Keith, G. A. Petersson, J. A. Montgomery, K. Raghavachari, M. A. Al-Laham, V. G. Zakrzewski, J. V. Ortiz, J. B. Foresman, J. Cioslowski, B. Stefanov, A. Nanayakkara, M. Challacombe, C. Y. Peng, P. Y. Ayala, W. Chen, M. W. Wong, J. L. Andres, E. S. Replogle, R. Gomperts, R. L. Martin, D. J. Fox, J. S. Binkley, D. J. Defrees, J. Baker, J. J. P. Stewart, M. Head-Gordon, C. Gonzales, and J. A. Pople, *GAUSSIAN 94*, Revision D.1 and D.4 (Gaussian, Inc., Pittsburgh, PA, 1995).
- ²⁴R. Bauer, S. J. Jensen, and B. Schmidt-Nielsen, *Hyperfine Interact.* **39**, 203 (1988).
- ²⁵*International Tables for Crystallography*, edited by A. J. C. Wilson, Mathematical, Physical and Chemical Tables Vol. C (Kluwer Academic, London, 1992), pp. 713–778.
- ²⁶J. M. Wiesenfeld, E. P. Ippen, A. Corin, and R. J. Bersohn, *J. Am. Chem. Soc.* **102**, 7256 (1980).